Critical evaluation of the 2D-CSIA scheme for distinguishing fuel oxygenate degradation reaction mechanisms

Mònica Rosell[1,4], Rafael González-Olmos[2,5], Thore Rohwerder[3], Klara Rusevova[2], Anett Georgi[2], Frank-Dieter Kopinke[2] and Hans H. Richnow[1]*

[1]Department of Isotope Biogeochemistry, [2]Department of Environmental Engineering and [3]Department of Environmental Microbiology

Helmholtz Centre for Environmental Research – UFZ

Permoserstrasse 15, 04318 Leipzig, Germany

Present addresses: [4]Grup de Mineralogia Aplicada i Medi Ambient, Departament de Cristal·lografia, Mineralogia i Dipòsits Minerals, Facultat de Geologia, Universitat de Barcelona, C/Martí i Franquès s/n, 08028 Barcelona, Spain

[5]Laboratori d'Enginyeria Química i Ambiental (LEQUIA), University of Girona, Faculty of sciences, Campus Montilivi s/n, 17071 Girona, Spain

* Corresponding author: Phone: +34-93 4021343, Fax: +34-93 4021340, e-mail: monica.rosell@ub.edu

Manuscript for submission in *Environmental Science and Technology*

22 **TOC Art**

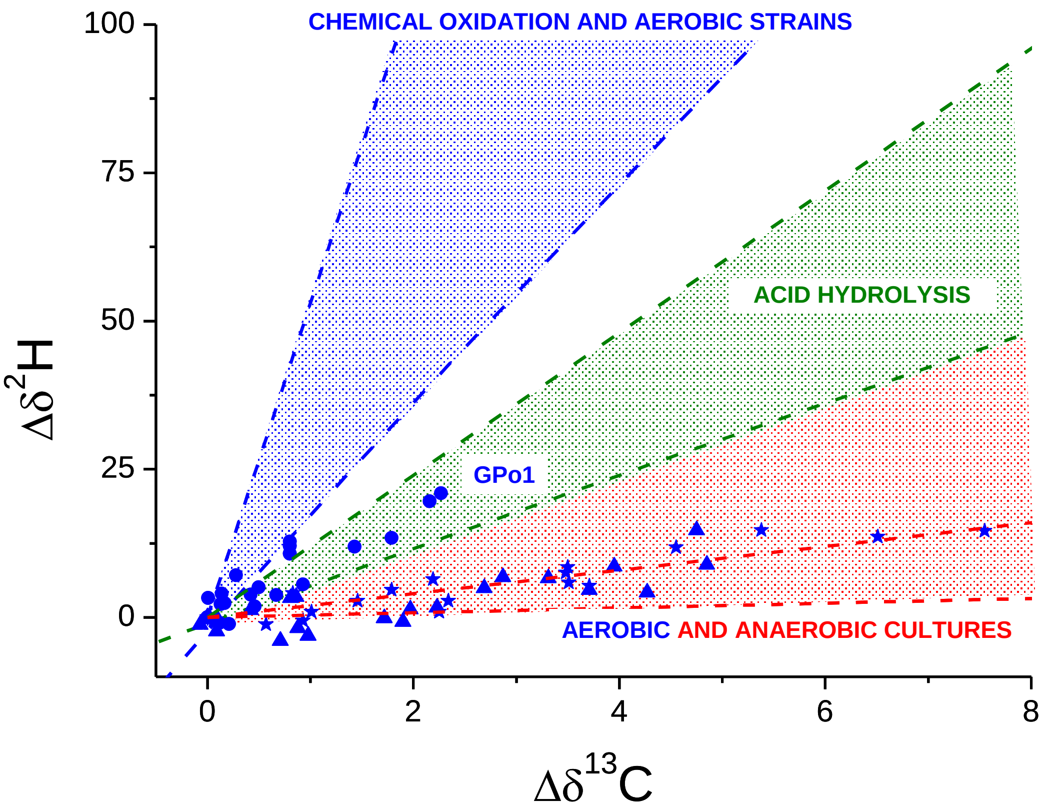

23

24

Abstract

Although the uniform initial hydroxylation of methyl *tert*-butyl ether (MTBE) and other oxygenates during aerobic biodegradation has already been proven by molecular tools, variations in carbon and hydrogen enrichment factors (ε_C and ε_H) have still been associated with different reaction mechanisms (McKelvie et al. *Environ. Sci. Technol*. **2009**, *43*, 2793-2799). Here, we present new laboratory-derived ε_C and ε_H data on the initial degradation mechanisms of MTBE, ethyl *tert*-butyl ether (ETBE) and *tert*-amyl methyl ether (TAME) by chemical oxidation (permanganate, Fenton reagents), acid hydrolysis and aerobic bacteria cultures (species of *Aquincola*, *Methylibium*, *Gordonia*, *Mycobacterium*, *Pseudomonas* and *Rhodococcus*). Plotting of $\Delta\delta^2$H/ $\Delta\delta^{13}$C data from chemical oxidation and hydrolysis of ethers resulted in slopes (Λ values) of 22 ± 4 and between 6 and 12, respectively. With *A. tertiaricarbonis* L108, *R. zopfii* IFP 2005 and *Gordonia* sp. IFP 2009, ε_C was low (<|-1|‰) and ε_H insignificant. Fractionation obtained with *P. putida* GPo1 was similar to acid hydrolysis and *M. austroafricanum* JOB5 and *R. ruber* DSM 7511 displayed Λ values previously only ascribed to anaerobic attack. The fractionation patterns rather correlate with the employment of different P450, AlkB and other monooxygenases, likely catalyzing ether hydroxylation via different transition states. Our data questions the value of 2D-CSIA for a simple distinguishing of oxygenate biotransformation mechanisms, therefore caution and complementary tools are needed for proper interpretation of groundwater plumes at field sites.

Keywords: MTBE; ETBE; TAME; CSIA (compound-specific stable isotope analysis); aerobic biodegradation; permanganate oxidation, Fenton reaction.

INTRODUCTION

Fuel oxygenates have been providing added value to the petrol industry for decades. Methyl *tert*-butyl ether (MTBE) has been used since the 1970's as gasoline additive due to its high octane number and its oxygen content which led to a reduction in emissions of exhaust pollutants. Today, in the era of climate change concerns and renewable energy ambitions, fuel oxygenates still play a major role. Since 2003, due to the promotion of the use of biofuels through tax incentives (Directive 2003/30/EC), some European MTBE refiners converted their plants to synthesize ethyl *tert*-butyl ether (ETBE) using bio-ethanol from agricultural feedstocks. Moreover, the new EU Renewable Energy Directive (2009/28/EC) contemplates the feasibility of bio-MTBE production using bio-methanol based on crude glycerin, a waste product from biodiesel production [1]. Overall, the estimated current annual production capacity of fuel ethers in Europe is approximately 6 million tones, split between almost 70 production plants and these compounds make up about 4% of the gasoline supply [2]. Despite the promotion of best practices for handling fuel ethers, their widespread use in gasoline caused contamination of groundwater tables worldwide [3, 4]. Similar to MTBE, ETBE and *tert*-amyl methyl ether (TAME) showed recently to cause odor and flavor problems making water sources unpalatable at very low concentrations (ETBE with 1–2 μg/L and MTBE and TAME from 7 to 16 μg/L) [5]. Mainly due to these public concerns, fuel oxygenate ethers are now partially or absolutely banned in some states of USA and substituted by ethanol [6]. However, drinking water resources will be threatened for a long time, as fuel oxygenates are recalcitrant to microbial attack particularly by the limited concentrations of oxygen typically found in fuel-contaminated aquifers [7].

In that respect, reliable methods for detecting *in situ* fuel oxygenates biodegradation and insights into the functioning of the responsible microorganisms are crucial for improving remediation technologies based on the activities of such degrading microorganisms. In recent years, compound-specific stable isotope analysis (CSIA) has been used as an important tool for monitoring biodegradation of organic contaminants in environmental systems [8, 9] and for characterizing the initial reaction mechanisms [10]. The reaction-dependent compound-specific isotope enrichment factors (ε) can be quantified using a modified form of the Rayleigh distillation equation under defined laboratory conditions [11] and converted to the apparent kinetic isotope effect (AKIE) to obtain information on the transition state of the bond cleavage reaction. The kinetic isotope effect (KIE) allows obtaining information on rate limitation and bond change of enzymatic reactions [12]. In environmental studies, isotope fractionation is used to characterize environmental processes and to predict reaction mechanisms, however, recent results on the diversity of isotopic fractionation during bacterial fuel oxygenate degradation question whether the extent of fractionation can be used to identify specific metabolic reactions [13].

The aerobic microbial MTBE degradation is initiated by a hydroxylation of the methyl group of the ether by a monooxygenase catalyzed reaction [14] and the breaking of the C-H bond would be expected to lead to similar carbon and hydrogen isotope effects. However, there are three different clusters of isotopic fractionation patterns found for aerobic MTBE degradation: (i) high fractionation of carbon and hydrogen was observed for *Methylibium* strains PM1 and R8 with ε_C and ε_H ranging from -2.0 to -2.4‰ and -33 to -40‰, respectively; (ii) similar carbon but higher hydrogen fractionation (ε_H = -100‰) was discovered for *Pseudonocardia tetrahydrofuranoxydans* K1; (iii) whereas much lower carbon fractionation ($\varepsilon_C \leq |-0.5|$‰) and practically non-detectable hydrogen fractionation was observed for *Aquincola tertiaricarbonis*

L108 and *Rhodococcus ruber* IFP 2001 [13, 15, 16]. Although this diversity in observed isotope effects questions the uniform hydroxylation step, studies on knockout mutants have clearly proven the involvement of monooxygenases in the initial attack of MTBE in the high-fractionating strain PM1 [17] and in the low-fractionating strains L108 and IFP 2001 [18, 19]. Therefore, low fractionation is likely associated with more efficient C-H bond breaking combined with rate determining non-fractionating steps involved in typically multistep processes of enzymatically catalyzed hydroxylation, thus masking the intrinsic isotope effect. However, as this suppression should equally affect isotopic fractionation of both elements, two-dimensional (2D)-CSIA graphs are thought to cancel these effects (when a reaction is committed to catalysis and become irreversible) and the ratio of hydrogen to carbon isotope fractionation should be able to distinguish between hydroxylation and other enzymatic reactions [10]. Considering analytical errors for determining low ε_H values, the fractionation observed with strains L108 and IFP 2001 may indeed give a similar slope as observed with strains PM1 and R8. However, it is clear that the two-dimensional scheme is not really applicable for very low isotopic fractionation. The different slopes (Λ) found for strain K1 (Λ = 48) vs. *Methylibium* spp. (Λ = 18) would lead to question the generally accepted assumption of a uniform hydroxylation mechanism for aerobic bacteria. Although the authors considered the high hydrogen enrichment factor of strain K1 consistent with the one they previously measured for abiotic oxidation of MTBE by permanganate (ε_H = -109‰), no information about ε_C or Λ was provided [20]. It is not clear, therefore, how a mechanism can be predicted for aerobic ether-degrading bacteria against alternative reaction mechanisms, such as the acid hydrolysis S_N1 (Λ = 11) and hydrolysis by (enzymatic) nucleophilic attack S_N2 suggested for the anaerobic degradation pathway (Λ = 1.2) [21]. In addition, the wide variability of enrichment factors ε_C from -0.37 to -2.29‰ and ε_H from <|-5| to -66‰ as well as Λ values in the range from 12 to 45 found in several aerobic mixed cultures from contaminated sites suggest the coexistence and activity of all the described degradation mechanisms within environmental microbial communities [15, 22-26]. These findings seriously complicate evaluation of *in situ* biodegradation of MTBE and other fuel oxygenates by 2D-CSIA. Therefore, additional studies are needed to elucidate how CSIA could be used for assessing fuel oxygenate biodegradation at groundwater contaminated sites.

Although there are isotope fractionation data for MTBE, there are few studies with ETBE and TAME. Therefore knowledge on the variability of isotopic fractionation among abiotic and biotic processes is needed for a proper evaluation of fuel oxygenate biodegradation employing CSIA for characterizing potentially contaminated sites in the future. For that purpose, we performed systematic work with a total of 10 pure strains (six of them were never tested before for isotopic fractionation studies) including *Aquincola*, *Methylibium*, *Gordonia*, *Mycobacterium*, *Pseudomonas* and *Rhodococcus* species which are able to grow aerobically on or cometabolically degrade MTBE, ETBE or TAME and compared their isotopic patterns with the results obtained in abiotic chemical oxidation experiments (permanganate vs. Fenton with $Fe^{2+/3+}$ and H_2O_2) as well as acid hydrolysis (HCl) in order to better understand their enzymatic mechanisms. Moreover, the present results could be useful to evaluate whether Fenton-like transformation of fuel oxygenates produces a significant isotopic fractionation pattern that can be used to monitor *in situ* chemical oxidation (ISCO), and to determine whether this pattern can be used to differentiate between biotic and abiotic transformation at a field site.

MATERIALS AND METHODS

Chemicals. All the chemicals and organic solvents were either purchased from Sigma-Aldrich (Munich, Germany) or Merck (Darmstadt, Germany) at analytical grade quality.

Abiotic oxidation reactions. Stoichiometric Fenton (with Fe^{2+}) and catalytic Fenton-like (with Fe^{3+}) reactions were carried out at 22 ± 2°C in 100-mL reactors, covered with foil paper in order to avoid photo-reactions, at pH 3 using solutions of $FeSO_4 \cdot 7\ H_2O$ or $Fe(NO_3)_3$, respectively, to oxidize 100 mg/L of each fuel oxygenate. In the stoichiometric Fenton reaction, equimolar concentrations of Fe^{2+} and H_2O_2 were used (10 mM of each). In order to avoid quenching of hydroxyl radicals by excess H_2O_2, H_2O_2 was added stepwise (1 mM each 5 min). In the catalytic Fenton-like reaction, an excess of H_2O_2 with respect to Fe^{3+} was used (0.03 mM Fe^{3+}; 100 mM H_2O_2). Permanganate oxidation reaction was also carried out at 22 ± 2°C in 100-mL reactors using a solution of 0.11 M of $KMnO_4$ to oxidize 250 mg/L of each fuel oxygenate. All the oxidation experiments were carried out with an individual fuel oxygenate compound, except one experiment with permanganate which was done with a mixture of 100 mg/L of MTBE and ETBE. For sampling, always 2-mL aliquots were taken in 5-mL vials over time. Sodium thiosulfate was added in order to stop the reaction (200 mM). Afterwards, the concentration of MTBE and ETBE was determined (see below). Samples were kept in the freezer at –20 ºC before analysis of isotopic fractionation. In addition, heterogeneous Fenton-like reactions with orthoferrites such as $BiFeO_3$ and $LaFeO_3$ in the presence of H_2O_2 at neutral pH and 22 ± 2°C were tested for MTBE and ETBE and can be found in the Supporting Information (SI).

Acid hydrolysis experiments. Hydrolysis was conducted in 100-mL serum bottles sealed with butyl rubber stoppers and incubated on a shaker at 30°C. The reaction was started by adding 100 µL of each pure fuel oxygenate to 100 mL of different dilutions of HCl (1, 3 or 5 M prepared from a Combi-Titrisol® 5M HCl, Merck, Darmstadt, Germany). At each sampling event, 3-mL aliquots were removed with a syringe and each 1-mL subsample was transferred into 20-mL headspace vials for duplicate headspace GC analysis [27] or one 10-mL vial for the stable isotope analysis, all of them containing 1 mL of the corresponding molarity of NaOH and cooled on ice to avoid losses during neutralization. Such a procedure served to quench the reaction and ensured that samples were free of volatile corrosive compounds.

Bacterial strains and cultivation conditions. *Aquincola tertiaricarbonis* L108 [28, 29] and *Methylibium* sp. R8 [16] were obtained from the strain collection of the UFZ department of Environmental Microbiology. *Methylibium petroleiphilum* PM1 [30, 31] were purchased from the American Type Culture Collection (ATCC BAA-1232). *Mycobacterium austroafricanum* IFP 2012, *Rhodococcus zopfii* IFP 2005, *Gordonia* sp. IFP 2009 and *Rhodococcus ruber* IFP 2001 were provided by F. Fayolle-Guichard (IFP Energies nouvelles, France). *Rhodococcus ruber* DSM 7511 was obtained from the German Collection of Microorganisms and Cell Cultures (DSMZ) and *Mycobacterium austroafricanum* JOB5 and *Pseudomonas putida* GPo1 from the collection of Institute Pasteur (CIP 105723 and CIP 105816, respectively). In general, the bacteria were grown in 1-L glass bottles filled with about 25% (v/v) mineral medium as described elsewhere [32] ensuring oxic conditions, 10% of inoculum (v/v) and appropriate growth substrate/s (see details in SI Table S1) on a rotary shaker at 30°C. After 5 days, cells were harvested by centrifugation (8500 rpm, 10 min at 4°C), washed with mineral salt solution and suspended at a high density. For resting-cell experiments, 60 mL of cell suspension were placed in 240-mL serum bottles, supplemented with vitamins and cobalt as for growing, 10-20 µL of each fuel oxygenate (MTBE, ETBE or TAME) and if necessary additional substrates for cometabolic degradation or enzyme inducers (see SI Table S1), closed immediately with butyl rubber stoppers and incubated as above. Control bottles were always prepared in parallel and were monitored for substrate concentrations and isotopic composition in order to evaluate abiotic losses or cross-contamination. Samples for substrate concentration, isotopic composition and pH were taken periodically according to Rosell et al. [27] until complete degradation (when possible).

Analytical methods. Monitoring of concentrations (fuel oxygenates and corresponding main degradation products) was performed using a headspace-gas chromatography system with flame ionization detector (HS-GC-FID) as described elsewhere [27] except for the chemical oxidation experiments where a mass spectrometer was used as detector [33]. Carbon and hydrogen stable isotopic composition of the fuel oxygenates were measured in all cases using gas chromatography-combustion-isotope ratio monitoring mass spectrometry systems (GC-C-IRM-MS) described in our previous work [16]. A Zebron ZB1 column (60 m length x 0.32 mm ID x 1 µm film thickness; Phenomenex, Aschaffenburg, Germany) was used for separation. Each sample was analyzed via headspace sampling in triplicate.

Stable isotope definitions and calculations. Carbon and hydrogen isotopic compositions are reported as $\delta^{13}C$ and $\delta^{2}H$ values in parts per thousand (‰) relative to Vienna Pee Dee Belemnite standard (V-PDB) and Vienna Standard Mean Ocean Water (V-SMOW), respectively

$$\delta[‰] = \left(\frac{R_{sample}}{R_{reference}} - 1\right) \times 1000 \qquad (1)$$

where R_{sample} and $R_{reference}$ are the atomic ratios of the heavy isotope to the light isotope ($^{13}C/^{12}C$ or $^{2}H/^{1}H$) in the sample and the international standard, respectively. A simplified Rayleigh equation for a closed system [11] was used to quantify the isotopic fractionation,

$$\ln\left(\frac{R_t}{R_0}\right) = \frac{\varepsilon}{1000} \cdot \ln\left(\frac{C_t}{C_0}\right) \qquad (2)$$

where the isotopic enrichment factor (ε) describes the relationship between changes in isotopic composition $R_t/R_0 = (\delta_t + 1000)/(\delta_0 + 1000)$ and the concentrations during the course of the experiment. When possible, 2D-CSIA was applied to the data sets. To correct for differences in the initial isotopic composition ($\delta^{13}C_0$ and $\delta^{2}H_0$) of MTBE, isotopic shifts for hydrogen ($\Delta\delta^{2}H$) and carbon ($\Delta\delta^{13}C$) were calculated by subtracting the isotopic signature at time *t* from the initial value ($\Delta\delta = \delta_t - \delta_0$). The slope of a linear regression of $\Delta\delta^{2}H$ vs. $\Delta\delta^{13}C$ describes the relationship between carbon and hydrogen fractionation (Λ).

$$\Lambda = \frac{\Delta\delta^{2}\mathrm{H}}{\Delta\delta^{13}\mathrm{C}} \approx \frac{\varepsilon_{\mathrm{H}}}{\varepsilon_{\mathrm{C}}} \qquad (3)$$

Each sample was measured at least in triplicate and all linear regression parameters including the 95% confidence intervals (CI) were obtained by the function “Linear Fit” using errors (standard deviation of measured data sets or corresponding propagated errors in both axes) as weight in OriginPro® 7.5.

RESULTS

Chemical oxidation of MTBE and ETBE. By means of the stoichiometric Fenton reaction (10 mM Fe^{2+} and stepwise addition of 10 mM of H_2O_2) ≥ 99% removal of MTBE and ETBE was achieved in less than 1 h (See SI Figure S1). The catalytic Fenton-like reaction (initiated with 0.03 mM Fe^{3+} and 100 mM H_2O_2) resulted in slower degradation of MTBE and ETBE (> 20 h required for ≥ 95% removal). ETBE reacts slightly faster than MTBE in both reaction systems. Fitting of the fuel oxygenate oxidation by pseudo-first order kinetics gives a ratio of the rate constants between MTBE and ETBE of 0.68 and 0.56 for the Fenton and Fenton-like reactions, respectively. This is in good agreement with the ratio of 0.59 previously reported with OHradicals [34]. In the reactions with permanganate, the removal of fuel oxygenates followed pseudo-first order kinetics (for 3 experiments R^2=0.93-0.995). The half-lives for MTBE and ETBE were 17.8 h and 0.81 h, respectively (see SI Figure S1). The ratio of the rate constants is 0.046. Permanganate selectively oxidizes the carbon atom adjacent to the ether bond under formation of an ester, whereby H-abstraction is the first step. In general, MnO_4^- has a higher reactivity with primary alkyl than with methyl carbon atoms in ethers [35, 36]. Thus ETBE is expected to degrade faster than MTBE, which is confirmed by our results.

The Rayleigh approach (equation 2) was applied to quantify the isotopic fractionation. The highest MTBE carbon and hydrogen isotopic fractionation during chemical oxidation of $\Delta\delta^{13}C$ = (15.6 ± 0.1)‰ and $\Delta\delta^{2}H$ = (387 ± 7)‰ was observed after 94% conversion by permanganate corresponding to ε_C and ε_H values of (-5.53 ± 0.04)‰ and (-109 ± 4)‰, respectively (see Table 1). In contrast, lower MTBE carbon and hydrogen isotopic fractionation was detected during the Fenton and Fenton-like oxidation reactions. Low values for the kinetic deuterium isotope effect (KDIE) in the range of 1.06 to 1.08 have been also reported for other reactions where H-abstraction from aliphatic carbon by hydroxyl radicals is considered as the predominant degradation pathway [37, 38]. In our study, no significant differences were found between ε_C (-1.2 ± 0.2)‰ vs. (-1.4 ± 0.1)‰ and ε_H (-29 ± 6)‰ vs. (-31 ± 9)‰ values obtained when using Fe^{2+} or Fe^{3+}, respectively. Moreover, when plotting the respective $\Delta\delta^{2}H$ vs. $\Delta\delta^{13}C$ values (equation 3) for the three tested oxidation reactions, comparable 2D-CSIA slopes, Λ, were obtained fitting into a range between 20 and 25 (mean Λ of 22 ± 4 for MTBE oxidation, R^2 = 0.94, n = 43, see Figure 1). Independently of the different reaction rates, analogous isotopic enrichment factors were found for MTBE and ETBE during each type of oxidation. A similar mean Λ of 23 ± 2 was also calculated for ETBE oxidation with a good correlation (R^2 = 0.9) when plotting all the values together (n = 11, Figure S2 in SI). Comparable results were also obtained when using orthoferrites as solid catalysts (see Table S2 in SI).

Acid hydrolysis of fuel oxygenates. Dissolved fuel oxygenate concentrations decreased exponentially with time in the eight batch experiments (R^2 = 0.82-0.9997) obtaining in all cases concomitant accumulation of main degradation products *tert*-butyl alcohol (TBA) and *tert*-amyl alcohol (TAA) from 46 to 94% of its parental compound (see SI Figure S2). At 30°C and in the presence of 5 M HCl, MTBE was hydrolyzed with a half-life of 0.64 h, whereas ETBE and TAME reacted even faster (0.35 and 0.03 h, respectively). In order to lower the hydrolysis rates for better monitoring of the reactions, further experiments were performed with lower HCl concentrations (3M and 1M). In this way, the half-life of MTBE at 1M HCl increased to 34 h, while ETBE and TAME required 17 and 8.5 h, respectively. For the three compounds, degradation >99% was achieved (see Table 1). Pronounced MTBE carbon and hydrogen isotopic fractionation of $\Delta\delta^{13}C = (28.58 \pm 0.05)$‰ and $\Delta\delta^{2}H = (106 \pm 12)$‰ was observed after 99.3% and 92% conversion, respectively, which corresponded to ε_C value of (-6.05 ± 0.03)‰ and ε_H value of (-43 ± 4)‰, when combining all data points (see Table 1). The data fitted the Rayleigh-type linear fractionation model with R^2 of 0.997 and 0.99, respectively, indicating that no significant difference in isotopic fractionation was detected at different acid concentrations. The corresponding 2D-CSIA slope, Λ, was 6.2 ± 0.5 (R^2 = 0.997) (equation 3). However, values closer to those previously published for MTBE were obtained for ETBE and TAME (see more details in Table 1) with Λ of 9.0 ± 0.3 (R^2 = 0.99) and 11.5 ± 0.2 (R^2 = 0.999), respectively.

Aerobic biodegradation of fuel oxygenates. In growing and resting-cell experiments with *A. tertiaricarbonis* L108, TAME was completely degraded without TAA accumulation and with low carbon fractionation of ε_C = (-0.4 ± 0.1)‰. Hydrogen fractionation was too low to be detectable with our methods. With *R. zopfii* IFP 2005 and *Gordonia* sp. IFP 2009, cometabolic MTBE and TAME degradation did not reach more than 30% after 2 weeks which was insufficient for determining isotopic fractionation. In contrast, ETBE degradation required only some hours. Both strains accumulated the ether metabolites TBA and TAA stoichiometrically. The ETBE carbon fractionation was low with ε_C = (-0.4 ± 0.1)‰ and (-0.62 ± 0.03)‰ for strains IFP 2005 and IFP 2009, respectively, and no significant ^{2}H enrichment was detected. The two *Methylibium* strains PM1 and R8 could grow on TAME and displayed identical carbon fractionation of ε_C = (-1.9 ± 0.1)‰. For two of the four batch experiments with strain PM1, the hydrogen fractionation was measured resulting in ε_H of (-52 ± 2)‰ and Λ of 25 ± 1 (R^2 = 0.86).

With *P. putida* GPo1, it was difficult to reach high degrees of degradation for MTBE and TAME (ETBE was not tested due to known low rates [39]). The best results were obtained after (i) growing the cells on glucose with dicyclopropylketone (DCPK) (the alternative growing substrate n-octane was difficult to wash out and inhibited temporarily fuel oxygenate degradation), (ii) several additions of glucose during the resting-cell experiments and (iii) the use of larger bottles (500 mL) for increasing the headspace volume and thus the oxygen supply. Under these conditions, the maximum degradation for MTBE and TAME reached 80 and 59%, respectively, along with the corresponding stoichiometric accumulation of TBA and TAA (*tert*-butyl formate, TBF, was not detected). A new MTBE fractionation pattern was discovered with intermediate carbon fractionation of ε_C = (-1.4 ± 0.1)‰ and low hydrogen fractionation of ε_H = (-11 ± 2)‰ resulting in a distinct Λ of 8 ± 1 (R^2 = 0.85). For TAME, the values were found in the same order of magnitude (see Table 2 for details).

With *M. austroafricanum* IFP 2012, degradation of the three fuel oxygenates was performed with TBA-grown resting cells. Although this strain is able to grow on MTBE, an inhibition of degradation at high concentration was observed by Francois et al. [40]. At an initial concentration of 480 µM (approx. 42 mg/L) when the degradation products (TBF and TBA) reached high concentrations, the MTBE degradation rate slowed down and stopped. Due to limited sensitivity of the isotope analysis, our resting-cells experiments were performed initially at MTBE concentrations 5 times higher (200 mg/L) compared to previous experiments [40]. We obtained a similar behavior and after 8 h when MTBE conversion was around 50%, TBF and TBA accumulated at about 4 and 44%, respectively, of initial parental concentration. At this point, the MTBE degradation slowed down and stopped at 66% after 9 days. Higher degradation levels were obtained in subsequent batch experiments by (i) reducing MTBE initial concentration to 100 mg/L (92% after the same incubation time) or/and (ii) adding acetate or glucose at 0.5 g/L at the beginning of the experiment (substantial reduction of experimental time and lower TBF concentrations). Comparable TAME degradation rates were observed under the same conditions whereas ETBE was always weakly degraded to a maximum 27% of the initial concentration. In all cases, the metabolites did not become degraded until the parental compound was almost depleted. In the case of the related strain *M. austroafricanum* JOB5, the fuel oxygenate degradation was strictly cometabolic in the presence of 0.5 g/L glucose. Although the main degradation products (TBA, TBF or TAA) were accumulated similarly to the experiment with strain IFP 2012; the degradation of TAME was around 5 times faster than of MTBE by strain JOB5. As with strains GPo1 and IFP 2012, ETBE was poorly degraded (4% in 50 days) and accompanied by TBA formation. Whereas the carbon isotopic fractionation of ε_C (-2.5 ± 0.1)‰ was similar to the values obtained with the *Methylibium* strains, the hydrogen isotopic fractionation was extremely low ($\varepsilon_H < |-5|$‰) leading to a very small Λ value when it was possible to calculate it (Λ = 1.7 ± 0.3 for strain JOB5, R^2 = 0.6). The same tendency was obtained for TAME degradation (see Table 2). Similar isotopic values were observed for *R. ruber* DSM 7511 during MTBE and TAME degradation. Strain DSM 7511 could not grow on ETBE, but it was able to degrade it completely in the presence of 0.5 g/L glucose.

DISCUSSION

Chemical model reactions. MTBE hydrogen fractionation was observed for all oxidation reactions tested (by permanganate, Fenton and Fenton-like reagents). However, the highest ε_H values were obtained by permanganate, fitting exactly the fractionation reported by Elsner et al. [20] for the same reaction. Interestingly, we observed also significant carbon fractionation for the latter process, while ε_C values for the Fenton reactions were much lower. Although individual enrichment factors for permanganate vs. Fenton reactions were different, they all gave the same Λ value. It was suggested that permanganate performs selective oxidation of C-H bonds next to an ether group, whereas Fenton's reagent is known to oxidize C-H bonds in a less selective fashion [20, 35]. The ratio of the rate constants for OH-radical attack at the methyl and *tert*-butyl groups of MTBE was reported to be 3:2 [41]. However, by means of CSIA, the exact mechanism can not be distinguished. The similar fractionation pattern with ETBE may point to a similar mechanism of C-H bond cleavage upon these reactions. Moreover, the use of iron in different oxidation states and species ($Fe^{2+/3+}$ and solid Fe(III)-oxide) has an insignificant effect on the bulk isotope fractionation of the ethers and, therefore, it is not possible to distinguish between these reactions . This might be explained by the fact that hydroxyl radicals are the dominant reactive species in all of the tested Fenton reactions (see further discussion on ferryl species in the SI).

It is not evident why our results of the acid hydrolysis as a model for S_N1 reactions with various concentrations of HCl at 30ºC were slightly different from those obtained by Elsner et al. [20] when using 2 M HCl at room temperature. However, the enrichment factors are in the same order of magnitude and differences of less than 1‰ (taking into account the 95% CI) might be attributed to lower precision obtained at a lower ether removal of 88%. Additional experiments are needed to understand the extent of variability associated with this reaction.

Bacterial isotopic fractionation challenges the simple use of the 2D-CSIA concept. The variability of carbon and hydrogen isotopic patterns observed during bacterial fuel ether degradation can only partially be explained by the chemical model reactions such as oxidation and hydrolysis (see Figure 1 as well as S2 and S3 in the SI). The MTBE pattern observed for the two *Methylibium* spp. (strains PM1 and R8) correlates with the assumed oxidation of the methyl group. In addition, the low carbon and insignificant hydrogen fractionation obtained with strains IFP 2005 and 2009 may be interpreted by masking effects due to more efficient hydroxylation catalysis, as has already been assumed for MTBE and ETBE attack by strains L108 and IFP 2001 [26, 27]. In contrast, the isotopic pattern discovered for strain K1 with such a high Λ value cannot be explained by oxidation reactions such as by permanganate, as it was suggested previously by comparing only the hydrogen fractionation [20], or by any other chemical reaction tested. In addition, from a mechanistic point of view, the Λ value (8 ± 1) found for strain GPo1 would be interpreted as S_N1 hydrolysis reaction mechanism (Λ from 5.7 to 12) [20]. This tendency was also observed for TAME degradation (see Figure S3 in SI). However, by testing OCT plasmid-deficient variants, it has unambiguously been proven that strain GPo1 employs a non-heme diiron alkane hydroxylase of the AlkB-type for attacking ether oxygenates [39]. More serious, MTBE isotopic patterns obtained with the aerobic strains IFP 2012 and JOB5 exhibited a Λ value fitting to the obtained values of an anaerobic enrichment culture (Λ = 1.2 ± 0.8) which was suggested to be an initial hydrolysis step via an S_N2 mechanism at the H_3C-O group [20, 21]. However, the formation of TBF during MTBE degradation by these strains clearly indicates the activity of hydroxylases in the initial fuel ether attack. Further, the involvement of another AlkB-type monooxygenase has been suggested for strains IFP 2012 and JOB5 as well as in other mycobacterial strains [40, 42, 43]. Likewise puzzling is the fractionation observed with strain DSM 7511. While the MTBE Λ value fitted to the anaerobic pathway slope (but also to the aerobic strain JOB5, see Figure 1), for ETBE a behavior closer to the acid hydrolysis (see Figure S2 in SI) was observed, suggesting different enzymatic mechanisms for the initial attack of each ether by this strain.

Biochemistry of C-H bond cleavage and transition state considerations. Considering the substantial evidence collected for the uniform hydroxylation step in the initial attack of fuel ethers by aerobic bacterial strains [14], hydrolysis reactions or other oxygen-independent processes can be ruled out. Hence, the interpretation of isotopic fractionation patterns only by the 2D-CSIA scheme without taking the extent of isotope fractionation into account is obviously misleading. For example, the significant diversity of fuel ether-attacking hydroxylase enzymes documented thus far cannot be ignored [14, 17, 44]. Consequently, accepting the well-known fact that different enzymes can catalyze identical reactions via different transition states (see recent review [45]) is a more straightforward explanation for the observed variability in isotopic fractionation.

The almost absence of isotopic fractionation observed for MTBE, ETBE and TAME degradation by strains L108, IFP 2001, IFP 2005 and IFP 2009 correlates well with the finding that in all these strains the P450 monooxygenase EthB is involved in the initial C-H bond breaking [19, 26, 46].

All four strains share EthB enzymes with nearly identical amino acid sequences, showing 98 to 99% identity. This high degree of similarity suggests nearly identical catalysis and substrate specificities allowing degradation of all ethers tested. Nevertheless, different transition states may still occur, as the interaction with the amino acid residues in the active site of the P450 enzymes likely vary for the different ether substrates. However, as C-H bond breaking is obviously not rate-limiting, the intrinsic isotope effects are nearly completely suppressed in all cases. Consequently, only slight variations in isotopic fractionation were observed.

Interpretation of the isotopic fractionation observed with strain K1 is more difficult. This strain [47] and the closely related strain *Pseudonocardia* sp. ENV478 [48] attack MTBE most likely by a four-component monooxygenase involved in degradation of tetrahydrofuran [13, 49], as only cells pre-grown on this cyclic ether compound show significant MTBE conversion to TBA. In addition, it has already been argued that the extremely high hydrogen fractionation found with strain K1 is consistent with the effects found for abiotic oxidation [13], supporting the involvement of a hydroxylation step. However, the published Λ value of about 50 is not reached by any of the tested oxidation reactions (Table 1). Hence, an effect simulating an "asymmetric masking" significantly affecting only the carbon isotopic fractionation must be postulated. Similar observations have been made with C-H bond breaking in the course of dehydrogenase reactions [50-52] and may suggest that chemical reactions should be taken with caution as a reference to predict mechanisms of enzymatic reactions. High deuterium fractionation was related to a transition state early in the reaction coordinate resembling more the substrate, while ^{13}C isotope effects were stronger in later transition states where the bond breaking is more advanced [50]. Therefore, an early transition state (maximum hydrogen but reduced carbon fractionation) might be the case for the catalysis of the hydroxylating enzymes involved in ether attack in strain K1.

Interestingly, Λ values obtained for ETBE and TAME with strain K1 were also close to 50, suggesting very similar transition states for all substrates.

Finally, we need a better understanding of the fractionation patterns observed with bacterial strains employing non-heme diiron alkane monooxygenases of the AlkB-type and possibly other types of hydroxylases. Strain PM1 uses the AlkB-type enzyme, MdpA, in the initial attack on MTBE [17]. This enzyme is also present in the closely related strain R8 and both strains show identical MdpA sequences [26]. In addition, both strains degrade MTBE with similar efficiency but are not able to attack ETBE [53]. Therefore, it is likely that MdpA is also involved in ether degradation in strain R8. Accordingly, the identical MTBE and TAME isotopic fractionation obtained for these strains would indicate similar transition states in MdpA catalysis in both strains. Potential masking of isotopic effects, if present, seem to affect equally carbon and hydrogen as Λ value fit the expected symmetric intrinsic isotopic effects of the C-H bond breaking. In contrast, totally different Λ values were obtained with the other strains where employment of AlkB-like monooxygenases has been suggested. This finding might be surprising at first glance, as all these enzymes belong to the same enzyme family and show significant sequence similarity including the four conserved motifs of iron-complexing histidine residues (see SI Figure S4). However, phylogenetic analysis has already revealed that MdpA, the AlkB from strain GPo1 and the mycobacterial enzymes form distinct groups [17, 54]. Particularly, amino acid residues of the second transmembrane domain directly interacting with the substrate deviate among the different AlkB enzymes [17, 55] (see TM helix 2 in SI Figure S4). Consequently, variations in substrate specificity are observed, as MdpA and the AlkB from strain GPo1 can only attack ethers, while the mycobacterial strains which likely also employ AlkB enzymes have a broader substrate spectrum including also the alcohols TBA and TAA. Highly likely, all these factors will influence transition state structure and, consequently, isotopic fractionation patterns. Significant differences between transition states have already been found for homologous enzymes with 87% sequence identity and 100% conserved catalytic sites [45]. In the case of fuel oxygenate degradation, with strains belonging to the same genus, i. e. *Methylibium*, *Pseudomonas* or *Mycobacterium*, similar fractionation patterns were obtained, indicating a correlation between functional and phylogenetic relationships. In this respect, it can be speculated whether the *Mycobacterium*-related Gram-positive strain DSM 7511 also employs the mycobacterial AlkB enzyme for ether degradation, as isotopic fractionation for MTBE corresponds well with the values obtained with strains IFP 2012 and JOB5. The higher ETBE $\Lambda = 7 \pm 1$ for the *Rhodococcus* strain may indicate the presence of a P450 hydroxylase, as this fractionation is in the same range of magnitude than the one of strain IFP 2001 ($\Lambda = 10 \pm 3$). Indeed, a common feature of many alkane degraders is that they contain multiple alkane hydroxylases with overlapping substrate ranges [56]. In particular, a study with 27 alkyl ether utilizing rhodococci strains proved that 26 of them contained multiple alkB genes encoding non-heme iron alkane monooxygenases as well as diverse P450 systems [57]. Since involvement of other hydroxylating enzymes (including AlkB monooxygenases) cannot be ruled out for strains IFP 2012 and JOB5 [43], isotopic fractionation patterns could also be the result of catalysis by multiple hydroxylases. However, identical 2D-CSIA slopes obtained with the latter strains correlate with the exclusive use of a single AlkB enzyme. The slightly different Λ values observed with strain DSM 7511 may also correspond to minor changes in transition states of the same enzyme due to molecular size differences of MTBE and ETBE.

Recommendations for biodegradation evaluation. Our study clearly shows that the 2D-CSIA scheme on its own cannot distinguish between aerobic and anaerobic fuel oxygenate degradation pathways (as it was previously assumed by Zwank et al. [58]) or between biotic and abiotic degradation in the case of ISCO applications at contaminated field sites. Our finding rather questions whether previous studies reporting low Λ values were really caused by anaerobic degradation processes. For example, Van Breukelen et al. [59] has criticized the conclusions of Zwank et al. [58] showing that biodegradation at the target field site was unlikely exclusively associated with anaerobic degradation based on his improved 2D-CSIA interpretation. Kuder et al. [21] plotted together isotopic data from nine different contaminated sites close to gasoline stations in the USA (Λ = 1.3), but anoxic conditions were only proved by microcosm experiments from one of them. Recently, Kujawinski et al. [60]classified as aerobic and anaerobic different sections of the same MTBE/ TAME contamination plume based on (i) the dissolved oxygen values (above or under 1 mg/L respectively) and (ii) the slope of the 2D-CSIA plot. However, some oxic samples fell clearly into the previously assumed anaerobic trend and some bacteria can effectively degrade MTBE below 0.5 mg/L of oxygen [27]. Although the detection of high carbon fractionation with ε_C values $\geq|-6|$‰ may still be indicative for anaerobic ether attack (see summary in Youngster et al. [25]), geochemical information e.g. redox conditions and availability of other electron acceptors now becomes crucial to validate interpretation of 2D-CSIA analysis. Further insights may be obtained in future studies when a third element (oxygen fractionation, $^{18}O/^{16}O$) is included in the CSIA concept. However, a routine methodology for the analysis of oxygen enrichment factors in bacterial degradation experiments and environmental aqueous samples by GC-C-IRMS has not been developed. More conveniently, 2D-CSIA should be applied together with molecular biological tools such as monitoring the expression of key enzymes [26, 61] or stable isotope probing approaches [24, 62] for a more reliable characterization of fuel oxygenate degradation. In addition, detection of key metabolites may be helpful. In this respect, it was recently discovered that strains PM1, R8 and L108 emit highly volatile alkenes during fuel oxygenate degradation [53]. As these compounds can easily be measured by simple GC devices, a further line of evidence on fuel ether biodegradation activities may be derived by analyzing gas samples from contaminated sites.

ACKNOWLEDGMENTS

We thank Carsten Vogt for helping in the obtaining of some strains and the initial cultivation performance; Françoise Fayolle-Guichard (IFP Energies nouvelles, Rueil-Malmaison, France) for providing us four IFP strains; U. Günther, M. Gehre, F. Bratfisch and S. Hinke for technical support in our isotope and cultivation laboratories.

M. Rosell was supported by a Beatriu de Pinós postdoctoral grant (2008 BP-A 00054) from the Autonomous Government of Catalonia (Agència de Gestió d'Ajuts Universitaris i de Recerca, AGAUR) and R. González-Olmos by a Marie Curie Intra-European Fellowship (PIEF-GA-2009-236583) within Marie Curie Mobility Actions of the European Commission 7th Framework Program.

Supporting Information Available

Details for bacterial cultivation (Table S1); plots for the degradation rate of the studied compounds in the chemical model reactions (permanganate, Fenton, Fenton-like and acid hydrolysis) (Figure S1); ETBE and TAME 2D-CSIA plots for the so far discovered initial reaction mechanisms (Figures S2 and S3); comparison of clustalW2 alignment of amino acid sequences of AlkB enzymes (Figure S4) as well as additional MTBE and ETBE isotopic results by heterogeneous Fenton-like reactions with orthoferrites $BiFeO_3$ and $LaFeO_3$ (Table S2) are provided in the Supporting Information. This information is available free of charge via the Internet at http://pubs.acs.org.

References

(1) The European Fuel Oxygenates Association (EFOA) Technological developments. http://www.efoa.eu/en/markets/ether-market-drivers-and-future-developments/technological-developments.aspx (November 2011).

(2) The European Fuel Oxygenates Association (EFOA) Ether Facts and Figures. http://www.efoa.eu/en/markets/ether-facts-and-figures.aspx (October 2011).

(3) Rosell, M.; Lacorte, S.; Barcelo, D. Occurrence and Fate of MTBE in the Aquatic Environment Over the Last Decade. In *Fuel Oxygenates*, Barceló, D., Ed. Springer-Verlag: Berlin Heidelberg, Germany, 2007; Vol. 5, Part R, pp 31–55.

(4) Fayolle-Guichard, F.; Durand, J.; Cheucle, M.; Rosell, M.; Michelland, R. J.; Tracol, J. P.; Le Roux, F.; Grundman, G.; Atteia, O.; Richnow, H. H.; Dumestre, A.; Benoit, Y. Study of an aquifer contaminated by ethyl tert-butyl ether (ETBE): site characterization and on-site bioremediation. *J. Hazard. Mater.* **2012**, *201- 202*, 236– 243.

(5) van Wezel, A.; Puijker, L.; Vink, C.; Versteegh, A.; de Voogt, P. Odour and flavour thresholds of gasoline additives (MTBE, ETBE and TAME) and their occurrence in Dutch drinking water collection areas. *Chemosphere* **2009**, *76* (5), 672-676.

(6) Weaver, J. W.; Exum, L. R.; Prieto, L. M. *Gasoline Composition Regulations Affecting LUST Sites*; EPA/600/R-10/001; Office of Research and Development, United States Environmental Protection Agency: Washington, DC, USA, January, 2010.

(7) Müller, R. H.; Rohwerder, T.; Harms, H. Carbon conversion efficiency and limits of productive bacterial degradation of methyl tert-butyl ether and related compounds. *Appl. Environ. Microbiol.* **2007**, *73* (6), 1783-1791.

(8) Meckenstock, R. U.; Morasch, B.; Griebler, C.; Richnow, H. H. Stable isotope fractionation analysis as a tool to monitor biodegradation in contaminated aquifers. *Journal of Contaminant Hydrology* **2004**, *75* (3-4), 215-255.

(9) Schmidt, T. C.; Zwank, L.; Elsner, M.; Berg, M.; Meckenstock, R. U.; Haderlein, S. B. Compound-specific stable isotope analysis of organic contaminants in natural environments: a critical review of the state of the art, prospects, and future challenges. *Analytical and Bioanalytical Chemistry* **2004**, *378* (2), 283-300.

(10) Elsner, M.; Zwank, L.; Hunkeler, D.; Schwarzenbach, R. P. A new concept linking observable stable isotope fractionation to transformation pathways of organic pollutants. *Environ. Sci. Technol.* **2005**, *39* (18), 6896-6916.

(11) Mariotti, A.; Germon, J. C.; Hubert, P.; Kaiser, P.; Letolle, R.; Tardieux, A.; Tardieux, P. Experimental-Determination of Nitrogen Kinetic Isotope Fractionation - Some Principles - Illustration for the Denitrification and Nitrification Processes. *Plant Soil* **1981**, *62* (3), 413-430.

(12) Northrop, D. B. The Expression of Isotope Effects on Enzyme-Catalyzed Reactions. *Annu. Rev. Biochem.* **1981**, *50*, 103-131.

(13) McKelvie, J. R.; Hyman, M.; Elsner, M.; Smith, C. A.; Aslett, D.; Lacrampe-Couloume, G.; Sherwood Lollar, B. Isotopic fractionation of MTBE suggests different initial reaction mechanisms during aerobic biodegradation. *Environ. Sci. Technol.* **2009**, *43* (8), 2793–2799.

(14) Lopes Ferreira, N.; Malandain, C.; Fayolle-Guichard, F. Enzymes and genes involved in the aerobic biodegradation of methyl tert-butyl ether (MTBE). *Appl. Microbiol. Biotechnol.* **2006**, *72* (2), 252-262.

(15) Gray, J. R.; Lacrampe-Couloume, G.; Gandhi, D.; Scow, K. M.; Wilson, R. D.; Mackay, D. M.; Sherwood Lollar, B. Carbon and hydrogen isotopic fractionation during biodegradation of methyl tert-butyl ether. *Environ. Sci. Technol.* **2002**, *36* (9), 1931-1938.

(16) Rosell, M.; Barcelo, D.; Rohwerder, T.; Breuer, U.; Gehre, M.; Richnow, H. H. Variations in 13C/12C and D/H enrichment factors of aerobic bacterial fuel oxygenate degradation. *Environ. Sci. Technol.* **2007**, *41* (6), 2036-2043.

(17) Schmidt, R.; Battaglia, V.; Scow, K.; Kane, S.; Hristova, K. R. Involvement of a novel enzyme, MdpA, in methyl tert-butyl ether degradation in *Methylibium petroleiphilum* PM1. *Appl. Environ. Microbiol.* **2008**, *74* (21), 6631-6638.

(18) Breuer, U.; Bäjen, C.; Rohwerder, T.; Müller, R. H.; Harms, H. In *MTBE degradation genes of an Ideonella-like bacterium L108*, 3rd European Conference on MTBE and Other Fuel Oxygenates, Antwerp, Belgium, 2007; Bastiaens, L., Ed. VITO: Antwerp, Belgium, 2007; p 103.

(19) Chauvaux, S.; Chevalier, F.; Le Dantec, C.; Fayolle, F.; Miras, I.; Kunst, F.; Beguin, P. Cloning of a genetically unstable cytochrome P-450 gene cluster involved in degradation of the pollutant ethyl tert-butyl ether by Rhodococcus ruber. *J. Bacteriol.* **2001**, *183* (22), 6551-6557.

(20) Elsner, M.; McKelvie, J.; Couloume, G. L.; Sherwood Lollar, B. Insight into methyl tert-butyl ether (MTBE) stable isotope Fractionation from abiotic reference experiments. *Environ. Sci. Technol.* **2007**, *41* (16), 5693-5700.

(21) Kuder, T.; Wilson, J. T.; Kaiser, P.; Kolhatkar, R.; Philp, P.; Allen, J. Enrichment of stable carbon and hydrogen isotopes during anaerobic biodegradation of MTBE: Microcosm and field evidence. *Environ. Sci. Technol.* **2005**, *39* (1), 213-220.

(22) Hunkeler, D.; Butler, B. J.; Aravena, R.; Barker, J. F. Monitoring biodegradation of methyl tert-butyl ether (MTBE) using compound-specific carbon isotope analysis. *Environ. Sci. Technol.* **2001**, *35* (4), 676-681.

(23) Lesser, L. E.; Johnson, P. C.; Aravena, R.; Spinnler, G. E.; Bruce, C. L.; Salanitro, J. P. An evaluation of compound-specific isotope analyses for assessing the biodegradation of MTBE at Port Hueneme, CA. *Environ. Sci. Technol.* **2008**, *42* (17), 6637-6643.

(24) Bastida, F.; Rosell, M.; Franchini, A. G.; Seifert, J.; Finsterbusch, S.; Jehmlich, N.; Jechalke, S.; von Bergen, M.; Richnow, H. H. Elucidating MTBE degradation in a mixed consortium using a multidisciplinary approach. *FEMS Microbiology Ecology* **2010**, *73*, 370–384.

(25) Youngster, L. K. G.; Rosell, M.; Richnow, H. H.; Häggblom, M. M. Assessment of MTBE biodegradation pathways by two-dimensional isotope analysis in mixed bacterial consortia under different redox conditions. *Appl. Microbiol. Biotechnol.* **2010**, *88* (1), 309-317.

(26) Jechalke, S.; Rosell, M.; Martinez-Lavanchy, P. M.; Perez-Leiva, P.; Rohwerder, T.; Vogt, C.; Richnow, H. H. Linking Low-Level Stable Isotope Fractionation to Expression of the Cytochrome P450 Monooxygenase-Encoding ethB Gene for Elucidation of Methyl tert-Butyl Ether Biodegradation in Aerated Treatment Pond Systems. *Appl. Environ. Microbiol.* **2011**, *77* (3), 1086-1096.

(27) Rosell, M.; Finsterbusch, S.; Jechalke, S.; Hübschmann, T.; Vogt, C.; Richnow, H. H. Evaluation of the Effects of Low Oxygen Concentration on Stable Isotope Fractionation during Aerobic MTBE Biodegradation. *Environ. Sci. Technol.* **2010**, *44* (1), 309-315.

(28) Lechner, U.; Brodkorb, D.; Geyer, R.; Hause, G.; Hartig, C.; Auling, G.; Fayolle-Guichard, F.; Piveteau, P.; Müller, R. H.; Rohwerder, T. *Aquincola tertiaricarbonis* gen. nov., sp nov., a tertiary butyl moiety-degrading bacterium. *International Journal Of Systematic And Evolutionary Microbiology* **2007**, *57*, 1295-1303.

(29) Müller, R. H.; Rohwerder, T.; Harms, H. Degradation of fuel oxygenates and their main intermediates by *Aquincola tertiaricarbonis* L108. *Microbiology-Sgm* **2008**, *154*, 1414-1421.

(30) Nakatsu, C. H.; Hristova, K.; Hanada, S.; Meng, X. Y.; Hanson, J. R.; Scow, K. M.; Kamagata, Y. *Methylibium petroleiphilum* gen. nov., sp nov., a novel methyl tert-butyl ether-degrading methylotroph of the *Betaproteobacteria*. *International Journal Of Systematic And Evolutionary Microbiology* **2006**, *56*, 983-989.

(31) Kane, S. R.; Chakicherla, A. Y.; Chain, P. S. G.; Schmidt, R.; Shin, M. W.; Legler, T. C.; Scow, K. M.; Larimer, F. W.; Lucas, S. M.; Richardson, P. M.; Hristova, K. R. Whole-genome analysis of the methyl tert-butyl ether-degrading beta-proteobacterium *Methylibium petroleiphilum* PM1. *J. Bacteriol.* **2007**, *189* (5), 1931-1945.

(32) Rohwerder, T.; Breuer, U.; Benndorf, D.; Lechner, U.; Müller, R. H. The alkyl tertiary butyl ether intermediate 2-hydroxyisobutyrate is degraded via a novel cobalamin-dependent mutase pathway. *Appl. Environ. Microbiol.* **2006**, *72*, 4128-4135.

(33) Gonzalez-Olmos, R.; Roland, U.; Toufar, H.; Kopinke, F. D.; Georgi, A. Fe-zeolites as catalysts for chemical oxidation of MTBE in water with H2O2. *Applied Catalysis B-Environmental* **2009**, *89* (3-4), 356-364.

(34) Karpel Vel Leitner, N.; Papailhou, A. L.; Croue, J. P.; Peyrot, J.; Dore, M. Oxidation of methyl tert-butyl ether (MTBE) and ethyl tert-butyl ether (ETBE) by ozone and combined ozone/hydrogen peroxide. *Ozone Science and Engineering* **1994**, *16* (1), 41-54.

(35) Schmidt, H. J.; Schafer, H. J. Oxidation of Hydrocarbons with Benzyl(Triethyl)Ammonium Permanganate. *Angewandte Chemie-International Edition in English* **1979**, *18* (1), 68-69.

(36) Waldemer, R. H.; Tratnyek, P. G. Kinetics of contaminant degradation by permanganate. *Environ. Sci. Technol.* **2006**, *40* (3), 1055-1061.

(37) Gonzalez-Olmos, R.; Holzer, F.; Kopinke, F. D.; Georgi, A. Indications of the reactive species in a heterogeneous Fenton-like reaction using Fe-containing zeolites. *Applied Catalysis a-General* **2011**, *398* (1-2), 44-53.

(38) Pignatello, J. J.; Liu, D.; Huston, P. Evidence for an additional oxidant in the photoassisted Fenton reaction. *Environ. Sci. Technol.* **1999**, *33* (11), 1832-1839.

(39) Smith, C. A.; Hyman, M. R. Oxidation of methyl tert-butyl ether by alkane hydroxylase in dicyclopropylketone-induced and n-octane-grown Pseudomonas putida GPo1. *Appl. Environ. Microbiol.* **2004**, *70* (8), 4544-4550.

(40) Francois, A.; Garnier, L.; Mathis, H.; Fayolle, F.; Monot, F. Roles of tert-butyl formate, tert-butyl alcohol and acetone in the regulation of methyl tert-butyl ether degradation by Mycobacterium austroafricanum IFP 2012. *Appl. Microbiol. Biotechnol.* **2003**, *62* (2-3), 256-262.

(41) Stefan, M. I.; Mack, J.; Bolton, J. R. Degradation pathways during the treatment of methyl tert-butyl ether by the UV/H2O2 process. *Environ. Sci. Technol.* **2000**, *34* (4), 650-658.

(42) Johnson, E. L.; Smith, C. A.; O'Reilly, K. T.; Hyman, M. R. Induction of methyl Tertiary butyl ether (MTBE)-oxidizing activity in Mycobacterium vaccae JOB5 by MTBE. *Appl. Environ. Microbiol.* **2004**, *70* (2), 1023-1030.

(43) House, A. J.; Hyman, M. R. Effects of gasoline components on MTBE and TBA cometabolism by Mycobacterium austroafricanum JOB5. *Biodegradation* **2010**, *21* (4), 525-541.

(44) Smith, C. A.; Hyman, M. R. Oxidation of gasoline oxygenates by closely related non-haem-iron alkane hydroxylases in Pseudomonas mendocina KR1 and other n-octane-utilizing Pseudomonas strains. *Environmental Microbiology Reports* **2010**, *2* (3), 426-432.

(45) Schramm, V. L. Enzymatic transition state theory and transition state analogue design. *J. Biol. Chem.* **2007**, *282* (39), 28297-28300.

(46) Malandain, C.; Fayolle-Guichard, F.; Vogel, T. M. Cytochromes P450-mediated degradation of fuel oxygenates by environmental isolates. *Fems Microbiology Ecology* **2010**, *72* (2), 289-296.

(47) Kämpfer, P.; Kohlweyer, U.; Thiemer, B.; Andreesen, J. R. Pseudonocardia tetrahydrofuranoxydans sp nov. *International Journal Of Systematic And Evolutionary Microbiology* **2006**, *56*, 1535-1538.

(48) Vainberg, S.; McClay, K.; Masuda, H.; Root, D.; Condee, C.; Zylstra, G. J.; Steffan, R. J. Biodegradation of ether pollutants by Pseudonocardia sp strain ENV478. *Appl. Environ. Microbiol.* **2006**, *72* (8), 5218-5224.

(49) Thiemer, B.; Andreesen, J. R.; Schrader, T. Cloning and characterization of a gene cluster involved in tetrahydrofuran degradation in Pseudonocardia sp strain K1. *Arch. Microbiol.* **2003**, *179* (4), 266-277.

(50) Botting, N. P. Isotope Effects In The Elucidation Of Enzyme Mechanisms. *Nat. Prod. Rep.* **1994**, *11* (4), 337-353.

(51) Scharschmidt, M.; Fisher, M. A.; Cleland, W. W. Variation Of Transition-State Structure As A Function Of The Nucleotide In Reactions Catalyzed By Dehydrogenases .1. Liver Alcohol-Dehydrogenase With Benzyl Alcohol And Yeast Aldehyde Dehydrogenase With Benzaldehyde. *Biochemistry* **1984**, *23* (23), 5471-5478.

(52) Hermes, J. D.; Morrical, S. W.; Oleary, M. H.; Cleland, W. W. Variation Of Transition-State Structure As A Function Of The Nucleotide In Reactions Catalyzed By Dehydrogenases .2. Formate Dehydrogenase. *Biochemistry* **1984**, *23* (23), 5479-5488.

(53) Schäfer, F.; Muzica, L.; Schuster, J.; Treuter, N.; Rosell, M.; Harms, H.; Müller, R. H.; Rohwerder, T. Formation of Alkenes via Degradation of tert-Alkyl Ethers and Alcohols by

Aquincola tertiaricarbonis L108 and Methylibium spp. *Appl. Environ. Microbiol.* **2011**, *77* (17), 5981-5987.

(54) Lopes Ferreira, N.; Mathis, H.; Labbe, D.; Frederic, M.; Greer, C. W.; Fayolle-Guichard, F. n-Alkane assimilation and tert-butyl alcohol (TBA) oxidation capacity in Mycobacterium austroafricanum strains. *Appl. Microbiol. Biotechnol.* **2007**, *75* (4), 909-919.

(55) van Beilen, J. B.; Smits, T. H. M.; Roos, F. F.; Brunner, T.; Balada, S. B.; Rothlisberger, M.; Witholt, B. Identification of an amino acid position that determines the substrate range of integral membrane alkane hydroxylases. *J. Bacteriol.* **2005**, *187* (1), 85-91.

(56) van Beilen, J. B.; Funhoff, E. G. Alkane hydroxylases involved in microbial alkane degradation. *Appl. Microbiol. Biotechnol.* **2007**, *74* (1), 13-21.

(57) Kim, Y. H.; Engesser, K. H.; Kim, S. J. Physiological, numerical and molecular characterization of alkyl ether-utilizing rhodococci. *Environmental Microbiology* **2007**, *9* (6), 1497-1510.

(58) Zwank, L.; Berg, M.; Elsner, M.; Schmidt, T. C.; Schwarzenbach, R. P.; Haderlein, S. B. New evaluation scheme for two-dimensional isotope analysis to decipher biodegradation processes: Application to groundwater contamination by MTBE. *Environ. Sci. Technol.* **2005**, *39* (4), 1018-1029.

(59) Van Breukelen, B. M. Extending the Rayleigh equation to allow competing isotope fractionating pathways to improve quantification of biodegradation. *Environ. Sci. Technol.* **2007**, *41* (11), 4004-4010.

(60) Kujawinski, D. M.; Stephan, M.; Jochmann, M. A.; Krajenke, K.; Haas, J.; Schmidt, T. C. Stable carbon and hydrogen isotope analysis of methyl tert-butyl ether and tert-amyl methyl ether by purge and trap-gas chromatography-isotope ratio mass spectrometry: Method evaluation and application. *Journal Of Environmental Monitoring* **2010**, *12* (1), 347-354.

(61) Baldwin, B. R.; Biernacki, A.; Blair, J.; Purchase, M. P.; Baker, J. M.; Sublette, K.; Davis, G.; Ogles, D. Monitoring Gene Expression To Evaluate Oxygen Infusion at a Gasoline-Contaminated Site. *Environ. Sci. Technol.* **2010**, *44* (17), 6829-6834.

(62) Busch-Harris, J.; Sublette, K.; Roberts, K. P.; Landrum, C.; Peacock, A. D.; Davis, G.; Ogles, D.; Holmes, W. E.; Harris, D.; Ota, C.; Yang, X.; Kolhatkar, A. Bio-Traps Coupled with Molecular Biological Methods and Stable Isotope Probing Demonstrate the In Situ Biodegradation Potential of MTBE and TBA in Gasoline-Contaminated Aquifers. *Ground Water Monitoring & Remediation* **2008**, *28* (4), 47-62.

Table captions

Table 1. Comparison of fuel oxygenates carbon and hydrogen isotopic enrichment factors (ε) and 2-D CSIA slopes (Λ) caused by different chemical oxidation reactions and acid hydrolysis experiments. When possible the respective 95% confidence intervals (± 95% CI) are provided.

Table 2. Carbon and hydrogen isotopic enrichment factors (ε) of fuel oxygenates and 2-D CSIA slopes (Λ) during biodegradation by aerobic pure strains grouped due to similar isotopic fractionation pattern. When possible the respective 95% confidence intervals (± 95% CI) are provided.

Table 1

Reaction	Target	ε_C [‰]	±95% CI [‰]	R^2	D [%]	N	ε_H [‰]	±95% CI [‰]	R^2	D [%]	N	Λ ± 95% CI	Reference
Chemical oxidation													
Oxidation by permanganate (n=1)	MTBE	?					-109	9	0.98	90	16	?	[20]
(n=3)	MTBE	-5.53	0.04	0.98	94	24	-109	4	0.92	94	24	20.1 ± 0.5	This study
(n=2)	ETBE	-5.2	0.1	0.996	99	6	-128	24	0.97	97	5	24 ± 4	This study
Oxidation Fenton (Fe^{2+}) (n=2)	MTBE	-1.2	0.2	0.90	99.1	11	-29	6	0.92	71	9	22 ± 4	This study
(n=1)	ETBE	-0.6	0.2	0.996	95	4	-18	-	0.82	66	3	23	This study
Oxidation Fenton (Fe^{3+}) (n=2)	MTBE	-1.4	0.1	0.95	97	12	-31	9	0.74	85	10	25 ± 5	This study
(n=1)	ETBE	-1.1	0.1	0.998	98	5	-18	-	1.00	92	3	17	This study
Acid hydrolysis (S_N1)													
2M HCl	MTBE	-4.9	0.6	0.995	88	6	-55	7	0.99	88	6	11 ± 1	[20]
5M (n=1) and 1M HCl (n=1)	MTBE	-6.05	0.03	0.997	99.3	17	-43	4	0.99	92	12	6.2 ± 0.5	This study
5M (n=1), 3M (n=1) and 1M HCl (n=1)	ETBE	-5.1	0.1	0.99	99	14	-47	2	0.96	99	14	9.0 ± 0.3	This study
5M (n=1), 3M (n=1) and 1M HCl (n=1)	TAME	-5.48	0.08	0.997	99	12	-66	2	0.8	97	9	11.5 ± 0.2	This study

n: number of experiments, N: number of data points; na: not analyzed or not applicable; ns: not significant; CI is 95% Confidence Interval; D%: maximum percentage of substrate initial/partial degradation (do not confuse with complete mineralization to CO_2) which could be analyzed for the corresponding isotopic composition taking into account different detection limits for carbon and hydrogen.

Table 2

Strain	Target	ε_C [‰]	±95% CI [‰]	R^2	D [%]	N	ε_H [‰]	±95% CI [‰]	R^2	D [%]	N	Λ ± 95% CI	Reference
Aquincola tertiaricarbonis L108*	MTBE	-0.48	0.05	0.94	96	34	ns (-0.2)	8	0.00	82	29	na	[16]
	ETBE	-0.67	0.04	0.93	98.9	69	-11.4	0.6	0.7	99.7	74	14 ± 1	[16]
(n=1)	TAME	-0.4	0.1	0.9	98	11	ns (+5)	11	0.5	94	7	na	This study
Rhodococcus ruber IFP 2001*	MTBE	-0.28	0.06	0.81	97	27	ns (+5)	20	0.14	88	24	na	[16]
	ETBE	-0.8	0.2	0.96	98	23	-10	2	0.8	98	23	10 ± 3	[16]
Gordonia sp. IFP 2009 (n=3)	ETBE	-0.62	0.03	0.995	98	15	ns (-10)	11	0.2	93	9	na	This study
Rhodococcus zopfii IFP 2005 (n=2)	ETBE	-0.4	0.1	0.98	91	7	na					na	This study
Methylibium petroleiphilum PM1	MTBE	-2.0 to -2.4	0.1 to 0.3	0.88 to 0.98	93	39	-33 to -37	4 to 5	0.90 to 0.99	80 to 90	26	18 ± 3	[10, 15]
(n=4)	TAME	-1.89	0.06	0.998	99	20	-52	2	0.9	91	10	25 ± 1	This study
Methylibium sp. R8*	MTBE	-2.3	0.1	0.98	98	40	-40	4	0.95	91	36	17 ± 1	[16, 24]
(n=2)	TAME	-1.9	0.1	0.99	99	12	na					na	This study
Pseudonocardia tetrahydrofuranoxydans K1	MTBE	-2.3	0.2	0.99		12	-100	10	0.99		11	48 ± 5	[13]
	ETBE	-1.7	0.2	0.99		9	-73	7	0.97		5	49 ± 4	[13]
	TAME	-1.7	0.3	0.99		5	-72	2	0.99		5	45 ± 4	[13]
Pseudomonas putida GPo1 (n=3)	MTBE	-1.4	0.1	0.91	80	28	-11	2	0.8	80	23	8 ± 1	This study
(n=3)	TAME	-1.1	0.2	0.9	59	32	-18	5	0.9	59	17	13 ± 3	This study
Mycobacterium austroafricanum IFP 2012 (n=5)	MTBE	-2.64	0.08	0.96	96	52	ns (+1)	2	0.02	92	43	na	This study
(n=5)	TAME	-2.16	0.05	0.995	96	41	ns (-0.2)	6	0.2	95	27	na	This study
Mycobacterium austroafricanum JOB5 (n=3)	MTBE	-2.50	0.04	0.994	96	31	-4.2	0.9	0.6	86	24	1.7 ± 0.3	This study
(n=3)	TAME	-2.12	0.05	0.998	99	20	ns (+3)	2	0.5	97	18	na	This study
Rhodococcus ruber DSM7511 (n=4)	MTBE	-2.48	0.06	0.997	99	27	-7	3	0.86	95	22	2.4 ± 0.8	This study
(n=2)	ETBE	-1.5	0.1	0.98	95	20	-11	2	0.8	95	20	7 ± 1	This study
(n=3)	TAME	-2.01	0.08	0.995	99	27	ns (-3)	3	0.05	85	22	na	This study

n: number of experiments, N: number of data points; na: not analyzed or not applicable; ns: not significant; CI is 95% Confidence Interval; D%: maximum percentage of substrate initial/ partial degradation (do not confuse with complete mineralization to CO_2) which could be analyzed for the corresponding isotopic composition taking into account different detection limits for carbon and hydrogen.

*Original data was recalculated according to Rosell et al. [27] and in the case of several experiments (e.g. growing and resting cells), the data was combined.

Figure captions

Figure 1. MTBE two dimensional plot of hydrogen versus carbon isotopic shifts for the so far discovered initial reaction mechanisms including (i) the mean slope (Λ value) for chemical oxidation (by plotting together permanganate and the two Fenton reactions in this study), (ii) the acid hydrolysis (S_N1-type, Λ range according to Elsner et al. [20] and our study), (iii) the S_N2-type hydrolysis suggested for an anaerobic enrichment culture [20, 21] although a Λ = 6 has been also reported for an anaerobic enrichment culture when adding syringic acid as co-substrate [25] (not shown) and (iv) the isotopic pattern discovered for strain K1 [13]. Linear regression curves (solid lines) allow comparison within the 95% confidence intervals (CI) (dashed lines). Measured values for strains GPo1 (circles), JOB5 (triangles) and DSM 7511 (stars) are shown. Previously studied strains PM1 and R8 fit to the chemical oxidation pattern (not shown) [15, 16]. Due to not measurable hydrogen fractionation, strains L108, IFP 2001 [16] and IFP 2012 are not shown.

Figure 1

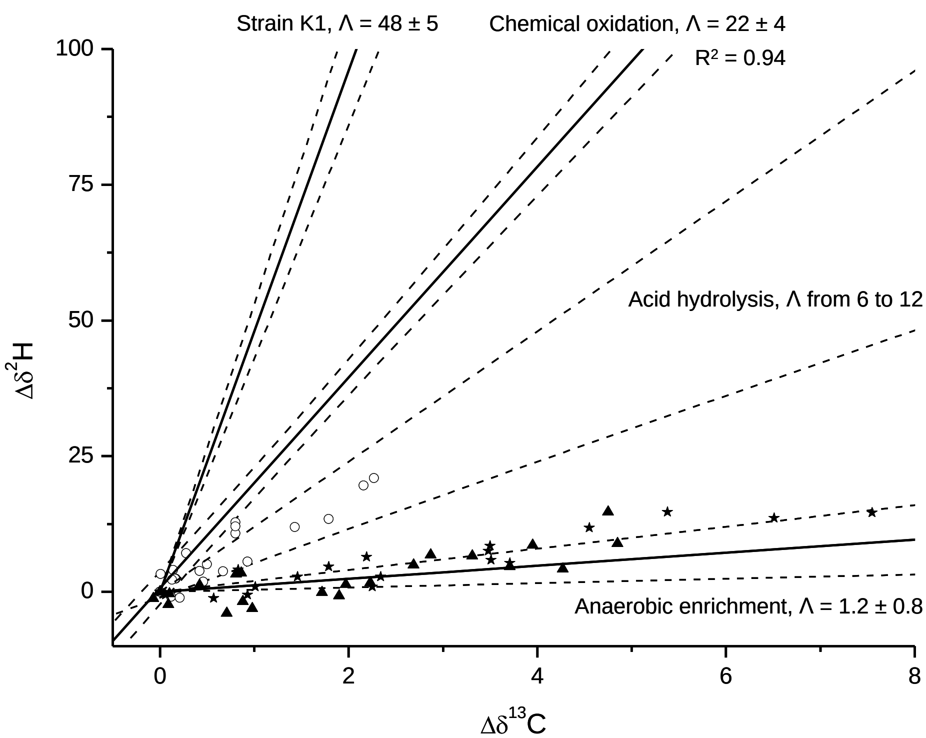
Strain K1, Λ = 48 ± 5
Chemical oxidation, Λ = 22 ± 4
R² = 0.94
Acid hydrolysis, Λ from 6 to 12
Anaerobic enrichment, Λ = 1.2 ± 0.8
100
75
50
25
0
0
2
4
6
8
Δδ²H
Δδ¹³C